Available online at www.sciencedirect.com
ScienceDirect
Journal of Solid State Chemistry 180 (2007) 1737–1742
JOURNAL OF SOLID STATE CHEMISTRY
www.elsevier.com/locate/jssc

Cation distribution and ferromagnetic exchange in the $YMn_{0.5}Co_{0.5}O_3$ perovskite investigated by neutron powder diffraction

M. Mouallem-Bahout[a,*], T. Roisnel[a], G. André[b], C. Moure[c], O. Peña[a]

[a]*Sciences Chimiques de Rennes, UMR 6226 CNRS, Université de Rennes 1, 263 avenue du général Leclerc, 35042 Rennes Cedex, France*
[b]*Laboratoire Léon Brillouin, (CEA-CNRS/Saclay), 91191 Gif sur Yvette Cedex, France*
[c]*Electroceramics Department, Instituto de Ceramica y Vidrio, CSIC, Campus de la Universidad Autonoma de Madrid, 28049 Cantoblanco, Madrid, Spain*

Received 8 November 2005; received in revised form 31 January 2007; accepted 26 February 2007
Available online 7 March 2007

Abstract

The synthesis and characterization of a polycrystalline $YMn_{0.5}Co_{0.5}O_{3-\delta}$ sample are reported. The oxygen-content, determined by the thermogravimetric method from complete reduction in flowing $5\%H_2/N_2$, shows some oxygen deficiency leading to the composition $YMn_{0.5}Co_{0.5}O_{2.87}$. Neutron powder diffraction shows some cation ordering at the six-coordinate site resulting in a monoclinic unit cell with $a = 5.241(1)$, $b = 5.594(1)$, $c = 7.468(1)$ and, $\beta \sim 90^\circ$ (space group $P2_1/n$) at 290 K. The sample undergoes a transition to a ferromagnetic phase at $T_c \sim 67$ K, with an ordered magnetic moment of 2.72(2) μ_B per formula unit aligned along [0 0 1].

Keywords: Manganites; Perovskite oxides; Thermogravimetry; Oxygen-content; Cation ordering; Neutron diffraction; Magnetic structure; Magnetic order

1. Introduction

Recent research into the phenomenon of colossal magnetoresistance (CMR) has increased interest in the structural and magnetic properties of mixed-metal perovskite manganites which can be formulated as $(Ln, A)MnO_3$, where *Ln* and *A* are usually lanthanide and alkaline-earth cations [1–3]. However, some authors investigated the structural and physical properties of *B*-site substituted manganites [4,5] attempting to obtain ferromagnetic behavior in double perovskites such as La_2NiMnO_6 ($LaNi_{0.5}Mn_{0.5}O_3$) and La_2CoMnO_6 ($LaCo_{0.5}Mn_{0.5}O_3$) by producing a 1:1 ordered cation array [6–8]. In our previous work including a study of the structural chemistry and magnetic properties of the $Y(Mn, Ni)O_3$ system, neutron powder diffraction (NPD) showed that the Mn and Ni cations in $YMn_{0.5}Ni_{0.5}O_3$ order in a 1:1 pattern [9,10]. At the same time, Bull et al. [11] and Dass et al. [12] demonstrated that the mixed transition ions order in La_2NiMnO_6 and La_2CoMnO_6, although annealing under high O_2-pressure was necessary to achieve full ordering in La_2CoMnO_6 [12].

In the present study, we aimed to ascertain the crystalline and magnetic structure of an $YMn_{0.5}Co_{0.5}O_{3-\delta}$ sample prepared by solid-state reaction and, compare our results to the data obtained on an $YMn_{0.5}Ni_{0.5}O_{3-\delta}$ sample [10]. Since standard X-ray is not convenient for such study, due to the similar scattering factors of Co and Mn [13] and, as anomalous powder X-ray is not adequate owing to comparable absorption energies of the 3d-ions, we used NPD to get better insight into the crystalline and magnetic structures of $YMn_{0.5}Co_{0.5}O_{3-\delta}$.

2. Experimental

A polycrystalline sample of $YMn_{0.5}Co_{0.5}O_{3-\delta}$ was prepared by solid-state reaction. Stoichiometric quantities of Y_2O_3, MnO_2 and CoO were intimately ground together by attrition milling, using isopropanol as liquid medium. The powders were pressed uniaxially into 1 cm-diameter pellets 2–3 mm thick and heated at 900 °C in air for a total of 24 h, with frequent regrinding, and finally at 1300 °C in air for 24 h, with intermittent regrinding. The progress of the reaction was monitored by X-ray powder diffraction,

*Corresponding author. Fax: +33 2 23236799.
E-mail address: mona.bahout@univ-rennes1.fr (M. Mouallem-Bahout).

0022-4596/$ - see front matter © 2007 Elsevier Inc. All rights reserved.
doi:10.1016/j.jssc.2007.02.022

and was deemed to be complete when further firing produced no change in the diffraction pattern.

A CPS 120 INEL diffractometer with a flat geometry, operating with Cu-Kα_1 radiation and equipped with a position sensitive detector was used to collect X-ray data over the angular range $5 \leqslant 2\theta(\text{deg}) \leqslant 120$. NPD experiments were carried out at the Orphée reactor (LLB-Saclay) using the G4.1 two-axis diffractometer ($\lambda = 2.4266$ Å, 800 cells multidetector extending over the angular range $10 \leqslant 2\theta(\text{deg}) \leqslant 90^\circ$). The data were analyzed by the Rietveld method as implemented in the Fullprof program [14,15], using the scattering lengths: $b(\text{Y}) = 0.775$, $b(\text{Mn}) = -0.375$, $b(\text{Co}) = 0.25$ and $b(\text{O}) = 0.581$ ($\times 10^{-12}$ cm). The background was modelled by means of a linear interpolation and, a Gaussian function was used to describe the instrumental and sample contributions to the peak profile. The fractional occupancies of the transition metals were initialized as 50% Mn and 50% Co at the 2*c*- and 2*d*-sites of the space group $P2_1/n$ corresponding to a fully disordered model before being allowed to vary with their sum constrained to be unity throughout the refinement. The room temperature refined values were held constant during the analysis of the lower temperature neutron diffraction data to allow the refinement of the magnetic structure. Thermogravimetric analysis was carried out using a Setaram-TGDTA92 Thermogravimetric Analyzer. Samples weighing approximately 50–70 mg contained in silica crucibles were placed in the apparatus which was previously purged with 5%H_2/N_2 and, were subsequently heated to 950 °C at a rate of 2 °C min^{-1} under the gas flow and held at this temperature for up to 30 min before being allowed to cool to room temperature under the gas flow, at the cooling rate of the furnace. The raw data were corrected from the crucible contribution according to measurement for the empty crucible under the same conditions.

3. Results and discussion

3.1. Oxygen content and thermogravimetric analysis

The thermogravimetric curve obtained for $YMn_{0.5}Co_{0.5}O_{3-\delta}$ is shown in Fig. 1, and compared to that obtained for a $YMn_{0.5}Ni_{0.5}O_{3-\delta}$ sample annealed under similar conditions. The reduction of both samples heated to 950 °C under the 5%H_2/N_2 flow proceeds to completion, as clear plateaux are visible in the weight loss. Inspection of the X-ray diffraction pattern of the residue after this treatment reveals the presence of Y_2O_3, MnO and Co(or Ni) metals. The absence of a residual perovskite phase confirms that the reduction was complete. The total weight loss for $YMn_{0.5}Co_{0.5}O_{3-\delta}$, $\Delta m = 7.25\%$ is similar to that obtained for $YMn_{0.5}Ni_{0.5}O_{3-\delta}$, $\Delta m = 7.42\%$, leading to similar oxygen-deficient compositions; $YMn_{0.5}Co_{0.5}O_{2.87}$ and $YMn_{0.5}Ni_{0.5}O_{2.89}$. To approach oxygen stoichiometry, various annealing of the Co-sample under 1-atm O_2-pressure have been performed in the range 1000−1300 °C,

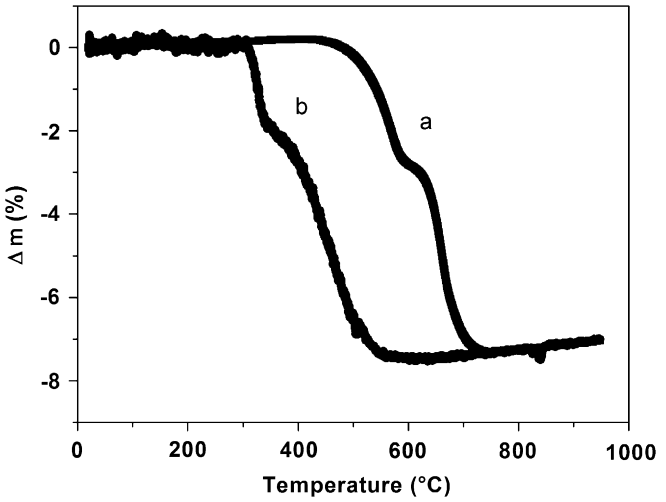

Fig. 1. Thermogravimetric curve of hydrogen reduction for $YMn_{0.5}Co_{0.5}O_{3-\delta}$ (a) in comparison to $YMn_{0.5}Ni_{0.5}O_{3-\delta}$ (b) in 5%H_2/N_2 flow; heating rate is 2 °C/min.

without significant increase of the oxygen-content. This result contrasts to that of the related $LaMn_{0.5}Co_{0.5}O_3$ perovskite which could be obtained stoichiometric under flowing O_2 [12].

Fig. 1 shows two gradual steps in the reduction process of $YMn_{0.5}Co_{0.5}O_{3-\delta}$ with onsets at temperatures $T_1 \sim 455$ °C and $T_2 \sim 590$ °C, higher than observed for the related $YMn_{0.5}Ni_{0.5}O_{3-\delta}$ sample, $T_1 \sim 305$ °C and $T_2 \sim 340$ °C.

3.2. Structural chemistry

Rietveld analysis of the X-ray powder diffraction patterns of $YMn_{0.5}Co_{0.5}O_{2.87}$ sample showed a single-phase, contrasting with the biphasic samples usually observed in the related $LaMn_{0.5}Co_{0.5}O_3$ and $LaMn_{0.5}Ni_{0.5}O_3$ samples [6,16]. Refinement of the data indicated that the space group was *Pbnm*(*Pnma*) orthorhombic with cell parameters $a = 5.241(1)$ Å, $b = 5.594(1)$ Å and $c = 7.468(1)$ Å. The absence of superlattice peaks, characteristic of cationic ordering was attributed to the reduced contrast between the scattering powers of Co/Mn constraining all the octahedral sites to be equivalent. However, the room temperature neutron diffraction pattern shows a weak reflection at $2\theta \sim 36.95^\circ$ ($d \sim 3.83$ Å) that could not be indexed in *Pbnm* but in monoclinic $P2_1/n$, resulting in some degree of cationic ordering over two distinguishable octahedral sites (Fig. 2), as reported for $YMn_{0.5}Ni_{0.5}O_{3-\delta}$ [10].

In order to determine the degree of ordering in $YMn_{0.5}Co_{0.5}O_{2.87}$, trial refinements with various starting values of the Mn/Co ions at the 2*c*- and 2*d*-sites converged to Mn(2*c*) = 0.34(1) and Mn(2*d*) = 0.66(1), reflecting some degree of cation ordering at the six-coordinate site. Since atomic order in double perovskites is usually governed by thermodynamic and kinetic parameters [17–19], various annealing of the $YMn_{0.5}Co_{0.5}O_{2.87}$ have been made in the

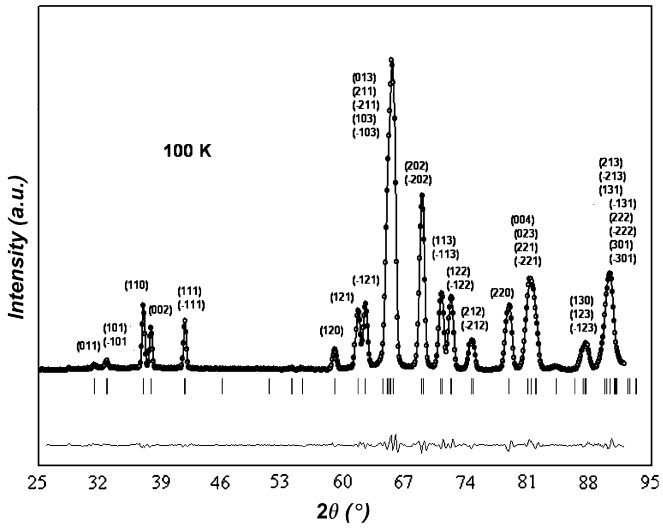

Fig. 2. Observed (•), calculated (−) and difference neutron diffraction patterns for $YMn_{0.5}Co_{0.5}O_{2.87}$ at room temperature. The tick marks indicate the reflections in $P2_1/n$ space group. The reflection (1 1 0) is forbidden in space group *Pbnm*(*Pnma*).

range 1000−1300 °C with different cooling rates, between 2 °C and 0.5 °C min^{-1} in order to maximize the ordering. No significant difference in the cationic distribution has been observed, and preference of Mn for the 2*d*- and Co for the 2*c*-sites was clear in all samples. The structural agreement parameters and selected bond distances are given in Tables 1 and 2 respectively, for the refinement shown in Fig. 2. Refinement of the oxygen occupancies confirms the oxygen content determined from thermogravimetric measurements. Fig. 3 displays the ideal structure of a $YMn_{0.5}Co_{0.5}O_3$ sample where Co and Mn ions alternate in the octahedra.

The oxidation state distribution in double perovskites has long been a matter of controversy [16–19]. Sonobe et al. [20] and Asai et al. [21] have reported ^{55}NMR data for $LaMn_{0.5}Ni_{0.5}O_3$ stating for a predominance of Mn^{IV} and Ni^{II}. In support of such an assignment, Blasse reported high temperature paramagnetic susceptibility data indicating that the preferred valences at high temperature appear to be Mn^{IV} and Ni^{II}, consistent with evidence of at least partial ordering of the two cations [7]. In opposition to this assignment of valences, Vasanthacharya et al. [22] used X-ray absorption and photoelectron spectroscopy to establish that in their disordered samples of $LaMn_xNi_{1-x}O_3$ with $x = 0.1$, 0.2 and 0.5, synthesized *via* a low temperature precursor route, Mn^{III} and low-spin Ni^{III} predominate. In addition, experimental values of the effective magnetic moments of $LaMn_xNi_{1-x}O_3$ samples were consistent with those calculated for xMn^{III} and low-spin $(1-x)Ni^{III}$. The conflicting observations obtained for the $LaMn_{0.5}Ni_{0.5}O_3$ samples produced by different workers appear to indicate that the relative stabilities of the valence states in such double perovskites, i.e., the position of the equilibrium represented in Eq. (1), depends upon the annealing temperature and degree of cation ordering, in turn dependent upon the cation oxidation states:

$$Mn^{IV} + Ni^{II} = Mn^{III} + Ni^{III}(LS). \quad (1)$$

Table 1
Atomic coordinates for $YMn_{0.5}Co_{0.5}O_{2.87}$ at room temperature, from analysis of the neutron diffraction data (NPD)[a]

Atom	*x*	*y*	*z*	*B* (Å^2)	Occupancy
Y	−0.0214(1)	0.0735(4)	0.2435(7)	0.32(7)	1
Mn/Co(2*d*)	0.5000	0.0000	0.0000	0.58(6)	0.33(4)
Mn/Co(2*c*)	0.5000	0.0000	0.5000	0.58(6)	0.17(4)
O1	0.1077(6)	0.4654(5)	0.2639(9)	0.98(4)	0.964 (4)
O2	0.6842(13)	0.2881(9)	0.0563(8)	0.98(4)	0.964 (4)
O3	0.6983(13)	0.3215(11)	0.4464(9)	0.98(4)	0.964 (4)

[a]Space group $P2_1/n$; $a = 5.2451(2)$ Å, $b = 5.6024(2)$ Å, $c = 7.4868(3)$ Å, $\beta = 89.85(6)^\circ$. The fractional occupancies of the octahedral-site refer to the proportion of Mn occupying the site. Goodness of fit parameter of $\chi^2 = 3.58$, $R_{wp} = 5.45$, $R_p = 5.41$.

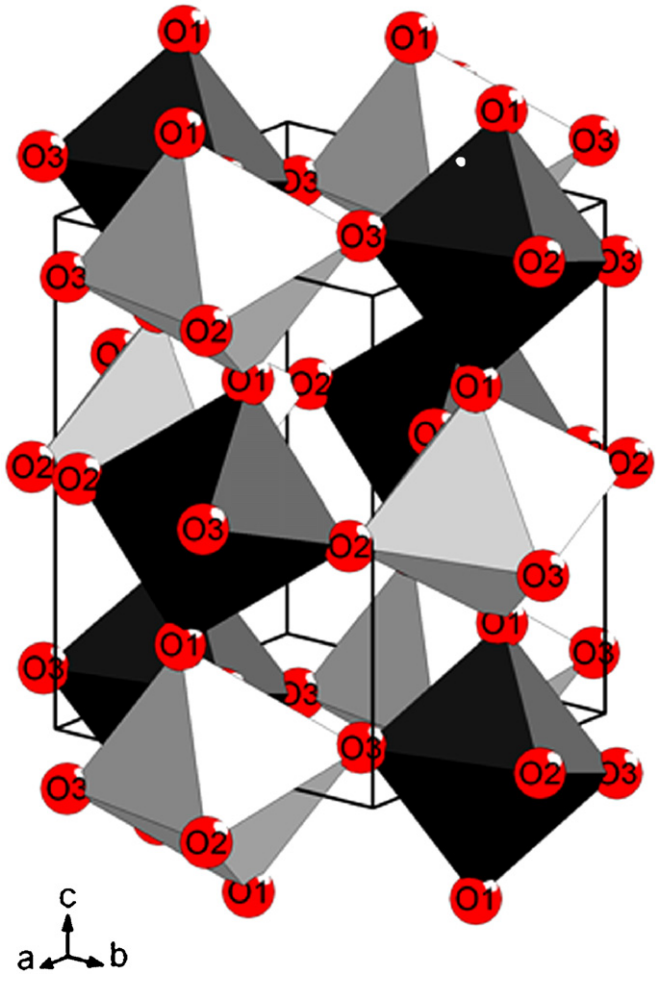

Fig. 3. Crystal structure showing the alternate occupation of the octahedra by Co and Mn ions for a completely ordered $YMn_{0.50}Co_{0.50}O_3$ perovskite. MnO_6 octahedra are shown in black and CoO_6 octahedra are coloured in white.

The $YMn_{0.5}Co_{0.5}O_{3-\delta}$ and $YMn_{0.5}Ni_{0.5}O_{3-\delta}$ compounds would adopt the same oxidation states as in the related perovskite La-phases. When the effective magnetic moment of $YMn_{0.5}Ni_{0.5}O_{3-\delta}$, obtained from fitting the high temperature susceptibility data to the Curie-law, $\mu_{eff} = 3.55\mu_B$ [23], is compared with values calculated on the basis of non-interacting spin-only moments for Mn^{III}/low-spin Ni^{III} ($3.67\mu_B$), Mn^{III}/high-spin Ni^{III} ($4.42\mu_B$) and *iii*) Mn^{IV}/Ni^{II} ($3.39\mu_B$), it results that μ_{eff} is consistent with the presence of either Mn^{III}/low-spin Ni^{III} or Mn^{IV}/Ni^{II} ions. However, the bond valence shell analysis of the NPD data gave ~1.920 Å and ~2.044 Å [10] for the mean bond lengths of Mn–O and Ni–O, respectively, leading to ionic radii of 0.52 Å for Mn and 0.64 Å for Ni, consistent with the presence of a majority of Ni^{II} and Mn^{IV} ions [24], although some Mn^{III} ions might exist to account for the oxygen deficiency.

An accurate estimation of the oxidation states of Co and Mn ions is difficult to obtain in the $YMn_{0.5}Co_{0.5}O_{2.87}$ sample from the $2c-O$ and $2d-O$ bond lengths, owing to the large antisite disorder. However, the configurations of the Co and Mn ions that can be considered are (i) Co^{II}-high spin/Mn^{IV}, (ii) Co^{III}-low spin/Mn^{III} and (iii) Co^{III}-high spin/Mn^{III}. The presence of a majority of Co^{II}-high spin/Mn^{IV} ions should be discarded in the present case, because the difference in size (0.745 Å/0.53 Å, respectively) and charge would have induced ordering at the B-sublattice. The magnetic data of $YMn_{0.5}Co_{0.5}O_{2.87}$ fitted to the Curie–Weiss law gave an effective moment value of $4.5\mu_B$ [25], lying between the spin-only moment for Co^{III}-high spin/Mn^{III} ($\mu_{eff} = 4.9\mu_B$) and Co^{III}-low spin/Mn^{III} ($\mu_{eff} = 3.5\mu_B$). Since high spin-Co(III) is unusual in octahedral oxygen environment, intermediate spin electronic configuration ($t_{2g}^5 e_g^1, S = 1$) might be assigned to Co in our $YMn_{0.5}Co_{0.5}O_{2.87}$ sample, in agreement with results reported for the related $LaCoO_3$ perovskite [26] (Table 2).

3.3. Magnetic properties

Perovskite oxides, ABO_3 are subject to indirect superexchange magnetic interactions. The oxygen ion in the perovskite crystal structure is coordinated by two *B*-ions that can magnetically interact. Since $YMn_{0.5}Co_{0.5}O_{2.87}$ is insulator [23,25], double exchange is not a factor and, the magnetic properties are governed by Goodenough–Kanamori rules [27,28] for the sign of the spin–spin superexchange interactions: (1) half-filled to empty orbital virtual spin transfer as in e^2-O-e^0, ferromagnetic coupling; (2) half-filled to half-filled orbital virtual charge transfer as in e^2-O-e^2 or t^3-O-t^3, antiferromagnetic coupling. In addition, (3) Jahn–Teller ions having a single electron in twofold-degenerate fluctuating *e*-orbital occupation as in e^1-O-e^1 give a three-dimensional ferromagnetic vibronic superexchange interaction [29–31]. The low-temperature NPD pattern (Fig. 4a, b) exhibits additional intensities superimposed over some nuclear peaks, indicative of a long-range ferromagnetic ordering. The Curie temperature T_c~67 K, determined *via* the temperature dependence of the (1 1 0) magnetic reflection (Fig. 5) is lower from that obtained from susceptibility measurements, T_c~75 K [25].

Table 2
Selected bond distances (Å) and angles (°) in $YMn_{0.5}Co_{0.5}O_{2.87}$ at room temperature from analysis of the neutron diffraction data

Y–O1	2.30(1)	(2*d*)–O1 (*x*2)	1.865(6)
Y–O1	3.14(3)	(2*d*)–O2 (*x*2)	1.928(6)
Y–O1	2.25(3)	(2*d*)–O3 (*x*2)	1.915(7)
Y–O2	2.41(2)	Mean (2*d*)–O	1.903(6)
Y–O2	2.35(1)		
Y–O2	2.69(2)	(2*c*)–O1 (*x*2)	2.065(7)
Y–O3	2.53(2)	(2*c*)–O2 (*x*2)	2.080(6)
Y–O3	2.21(2)	(2*c*)–O3 (*x*2)	2.118(6)
Y–O3	2.57(2)	Mean (2*c*)–O	2.088(6)
Mean Y–O	2.49(2)		
	(2*c*)–O1–(2*d*)	144.5(3)	
	(2*c*)–O2–(2*d*)	146.4(2)	
	(2*c*)–O3–(2*d*)	144.1(3)	

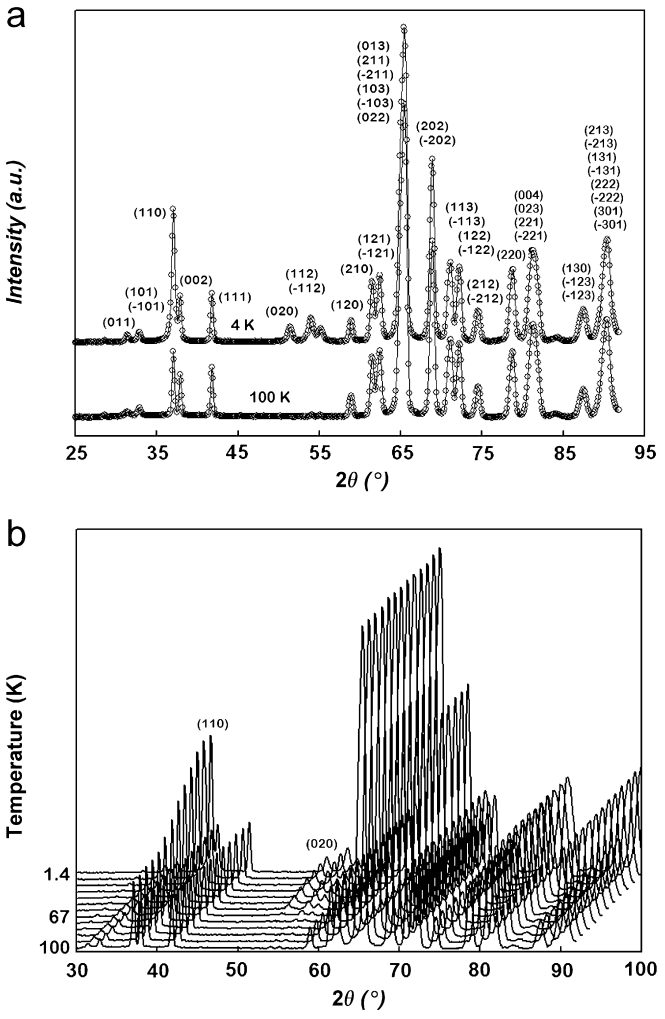

Fig. 4. (a)Neutron powder diffraction patterns for $YMn_{0.5}Co_{0.5}O_{2.87}$ at 1.4 K (upper diagram) and 100 K (lower diagram), (b) 3D thermograms for $YMn_{0.5}Co_{0.5}O_{2.87}$ between 1.4 and 100 K, the temperature dependence of the (1 1 0) peak is indicative of the ferromagnetic ordering.

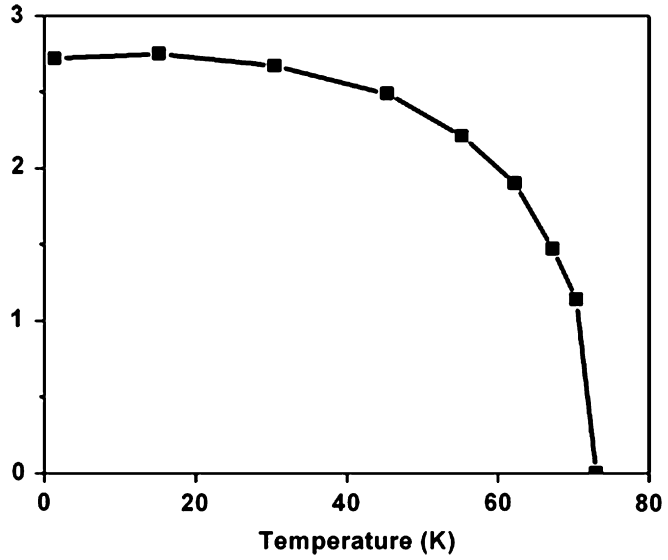

Fig. 5. Temperature dependence of the (1 1 0) magnetic line for $YMn_{0.50}Co_{0.50}O_{2.87}$.

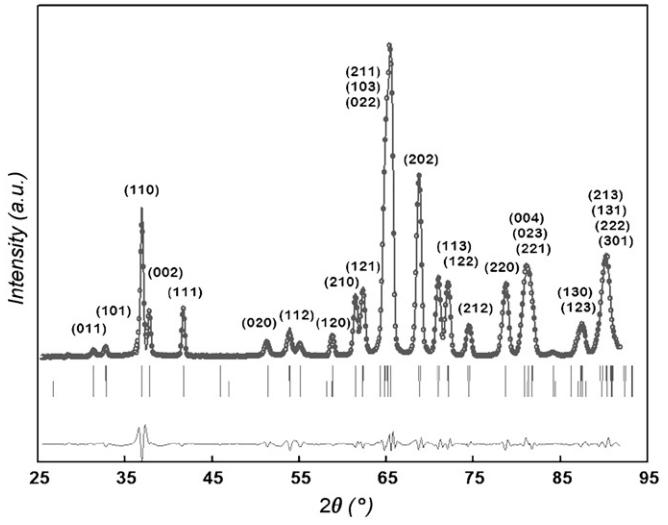

Fig. 6. Neutron diffraction patterns for $YMn_{0.5}Co_{0.5}O_{2.87}$ at 1.4 K. The first row of tick marks indicates the nuclear reflections in $P2_1/n$ space group, the second row indicates the magnetic reflections in P_1; $\chi^2 = 21$, $R_{wp} = 6.19\%$, $R_p = 5.67\%$.

Such difference might be due either to different oxygen contents resulting from different annealing conditions or to magnetic measurements performed using different techniques.

Refinement of the neutron data at 1.4 K, assuming a mean magnetic ion at the 2*c*- and 2*d*-sites (Fig. 6), shows that the spins couple ferromagnetically along [0 0 1] with $M_z \sim 3.26(6)\ \mu\beta$ and 2.14(4) $\mu\beta$ at the 2*c*- and 2*d*-sites, respectively, leading to a saturated magnetic moment $M_s \sim 2.72\mu_B$ per mean 3*d*-ion. Although M_s could not be accurately compared to that determined from magnetization [25] because of different annealing conditions between the samples, both magnetic moments are reduced fraction of that to be expected from a fully aligned array of Mn/Co cations. This result might arise from the presence of a large antisite disorder producing antiferromagnetic Mn–O–Mn and Co–O–Co bonds.

Ordering of Mn^{IV} and Ni^{II} ions in $YMn_{0.5}Ni_{0.5}O_{2.89}$, gives ferromagnetic e^0-O-e^2 coupling via σ-bonding in agreement with a magnetic structure consisting of collinear Mn^{IV} and Ni^{II} (F_x0F_y) sublattices with inter-planes ferromagnetic coupling [10]. However, since the $YMn_{0.5}Co_{0.5}O_{2.87}$ sample is poorly ordered and, the interaction between $Co^{3+}(t_{2g}^6e_g^0)$ ions or $Mn^{3+}(t_{2g}^3e_g^1)$ ions mutually are antiferromagentic, the ferromagnetic behavior might be explained by the presence of intermediate-spin-Co^{III} ions. Indeed, intermediate-spin Co^{III} ($t_{2g}^5e_g^1$) and Mn^{III} ($t_{2g}^3e_g^1$) are Jahn–Teller ions with single electrons in twofold-degenerate fluctuating *e*-orbital, strongly stabilized by three-dimensional ferromagnetic coupling due to e^1-O-e^1 vibronic superexchange, as it has been reported for the related $LaMn_{0.5}Co_{0.5}O_{3-\delta}$ [30].

4. Conclusion

A single perovskite phase $YMn_{0.5}Co_{0.5}O_{2.87}$ has been prepared by solid-state reaction. Neutron diffraction data allowed us to reach the degree of cation order and to assign the oxidation state (III) for the Co and Mn cations. The ferromagnetic structure consists of magnetic moments lying along the *c*-axis. For a better correlation between the structural and magnetic properties and to get better insight in cation order phenomena over a length scale shorter than that scaled in diffraction experiments, EXAFS and electron microscopy experiments are in progress.

References

[1] C. Zener, Phys. Rev. 82 (1951) 403.
[2] J.M.D. Coey, M. Viret, S. Von Molnar, Adv. Phys. 48 (1999) 167.
[3] S.W. Cheong, H.Y. Huang, in: Y. Tokura (Ed.), Colossal Magnetoresistive Oxides, Singapore, Gordon and Breach, 2000.
[4] J.B. Goodenough, Phys. Rev. 100 (1955) 564.
[5] J.B. Goodenough, J. Phys. Chem. Solids 6 (1958) 287.
[6] J.B. Goodenough, A. Wold, R. Arnott, N. Menyuk, Phys. Rev. 124 (1961) 373.
[7] G. Blasse, J. Phys. Chem. Solids 26 (1965) 1969.
[8] K. Asai, K. Fujiyoshi, N. Nishimori, Y. Satoh, Y. Kobayashi, M. Mizoguchi, J. Phys. Soc. Jpn 67 (1998) 4218.
[9] Structural and magnetic neutron diffraction study of the perovskite manganites $RENi_{0.5}Mn_{0.5}O_3$ (*RE* = La, Nd, Y) and $YNi_{0.25}Mn_{0.75}O_3$, M. Mouallem-Bahout, T. Roisnel, F. Bourée, G. André, C. Moure, O. Peña, in: 14th International Conference on the Solid Compounds of the Transition Elements, 11 July 2003, Cherbourg, France, 2003.
[10] M. Mouallem-Bahout, T. Roisnel, G. André, D. Gutiérrez, C. Moure, O. Peña, Solid State Commun. 129 (2004) 255.
[11] C.L. Bull, D. Gleeson, K.S. Knight, J. Phys. Condens. Matter 14 (2003) 4927.
[12] R.I. Dass, J.B. Goodenough, Phys. Rev. B 67 (2003) 014401.
[13] J.A. Ibers, D.H. Templeton, B.K. Vainshtein, G.E. Bacon, K. Lonsdale, in: C.H. Macgillavry, G.D. Rieck, K. Lonsdale (Eds.), International Tables of X-ray Crystallography, vol. III, Section 3.3, Birmingham, England, 1962, p. 201.

[14] J. Rodriguez-Carvajal, Powder diffraction, in: Satellite Meeting of the 15th Congress of IUCr, Toulouse, France, 1990, p. 127.
[15] J. Rodriguez-Carvajal, Physica B 192 (1992) 55.
[16] V.L. Joseph Joly, P.A. Joy, S.K. Date, Phys. Rev. B 65 (2002) 184416.
[17] I.O. Troyanchuk, M. Samsonenko, N. Kasper, 0H. Szymczak, A. Nabialek, J. Phys. Condens. Matter 9 (1997) 287.
[18] A. Wold, R.J. Arnold, J.B. Goodenough, J. Appl. Phys. 29 (1958) 387.
[19] O. Peña, D. Gutierrez, P. Durán, C. Moure, Bol. Soc. Esp. Ceram. Vidrio 43 (2004) 732.
[20] M. Sonobe, A. Kichizo, J. Phys. Soc. Jpn 61 (1992) 4193.
[21] K. Asai, H. Sekizawa, S. Iida, J. Phys. Soc. Jpn 47 (1979) 1054.
[22] N.Y. Vasanthacharya, P. Ganguly, J.B. Goodenough, C.N.R. Rao, J. Phys. C Solid State Phys. 17 (1984) 2745.
[23] O. Peña, M. Mouallem-Bahout, D. Gutiérrez, J.F. Fernández, P. Durán, C. Moure, J. Phys. Chem. Solids 61 (2000) 2019.
[24] R.D. Shannon, Acta Crystallogr. A32 (1976) 751.
[25] D. Gutiérrez, O. Peña, K. Ghanimi, P. Durán, C. Moure, J. Phys. Chem. Solids 63 (2002) 1975.
[26] K. Asai, P. Gehring, H. Chou, G. Shirane, Phys. Rev. B 40 (1989) 10982.
[27] J.B. Goodenough, Phys. Rev. 100 (1955) 564.
[28] J. Kanamori, J. Phys. Chem. Solids 10 (1959) 87–98.
[29] J.B. Goodenough, R.I. Dass, J.S. Zhou, Solid State Sci. 4 (2002) 297.
[30] G.T.K. Fey, W. Li, J.R. Dahn, J. Electrochem. Soc. 141 (1994) 2274; J.M. Paulsen, C.L. Thomas, J.R. Dahn, J. Electrochem. Soc. 147 (2000) 861.
[31] Y. Tokura, Y. Okimoto, S. Yamaguchi, H. Taniguchi, T. Kimura, H. Takagi, Phys. Rev. B 58 (1998) R1699.